INTERNATIONAL JOURNAL FOR NUMERICAL METHODS IN FLUIDS, VOL. 16, 173–186 (1993)

A LINEARIZED RIEMANN SOLVER FOR THE STEADY SUPERSONIC EULER EQUATIONS

ELEUTERIO F. TORO AND CHENG-CHIANG CHOU

Department of Aerospace Science, College of Aeronautics, Cranfield Institute of Technology, Cranfield, Beds MK43 OAL, U.K.

SUMMARY

A very simple linearization of the solution to the Riemann problem for the steady supersonic Euler equations is presented. When used locally in conjunction with the Godunov method, computing savings by a factor of about four relative to the use of exact Riemann solvers can be achieved. For severe flow regimes, however, the linearization loses accuracy and robustness. We then propose the use of a Riemann solver adaptation procedure. This retains the accuracy and robustness of the exact Riemann solver and the computational efficiency of the cheap linearized Riemann solver. Numerical results for two- and three-dimensional test problems are presented.

KEY WORDS Supersonic flow Linearized Riemann solver Space marching Godunov-type methods

1. INTRODUCTION

Godunov-type methods or Riemann-problem-based shock-capturing methods are a large subset of high-resolution methods. They have made a significant impact in Computational Fluid Dynamics (CFD) in the last decade.[1] Their initial success for compressible, time-dependent inviscid flows with shock waves has been extended to other hyperbolic flows such as steady supersonic flows[2,3] and shallow water flows[4] and, more recently, to parabolic flows such as the compressible Navier–Stokes equations.[5,6] These methods are (a) conservative, which means that computed discontinuous waves have correct positions, (b) shock-capturing, which means that a single numerical method is used throughout the flow field, and (c) Total-Variation-Diminishing (or TVD), which means that for the one-dimensional time-dependent and two-dimensional steady supersonic cases they are at least second-order-accurate almost everywhere; for other cases it is difficult to assess the overall accuracy, but numerical evidence suggests that this might be preserved. By virtue of the TVD condition these schemes do not exhibit the spurious oscillations near high gradients (e.g. shocks) that are typical of other methods such as those of the artificial viscosity type. Godunov-type methods are also very robust and by virtue of property (c) there are no arbitrary computing parameters as is the case in traditional artificial viscosity methods. One disadvantage relative to these methods, however, is that algorithms are more complex and more demanding on processing power, although this latter aspect needs qualifying. Once all computational parameters in a typical artificial viscosity method have been fixed, the computation of the solution to a specified problem may take about a third of the time required by a Riemann-problem-based method. However, the computing and human cost involved in the determination of optimal values for the computational parameters in the artificial viscosity method can be

0271–2091/93/030173–14$12.00

Received November 1991
Revised September 1992

significant. This aspect should be considered when assessing the computational efficiency of numerical methods.

Further research on Riemann-problem-based methods aimed at reducing computing costs and simplifying algorithms is, however, still needed. The solution of the Riemann problem lies at the centre of the computational expense and algorithm complexity. For realistic computations the Riemann problem is solved billions of times. For the case of time-dependent ideal flows there are several fairly simple approximate Riemann solvers. Even current exact Riemann solvers are quite competitive, but for steady supersonic flows the exact Riemann solver is significantly more complex than its counterpart in time-dependent gas dynamics. Approximate Riemann solvers have been presented by Pandolfi[2] and Roe[7], but the experience in applying these to realistic problems is more limited than that in time-dependent problems.

The contents of this paper concern the reduction of both the computing cost and algorithm complexity of Riemann-problem-based methods for steady supersonic flows in two and three dimensions. We present an approximate Riemann solver based on a local linearization of the equations in primitive variable form. The solution is direct and involves few and very simple arithmetic operations. For flows containing shock waves of moderate strength, i.e. pressure ratios of about 10, the numerical results are very accurate and the algorithms are simple and robust.

For severe flow regimes we advocate the adaptive use of the present Riemann solver in conjunction with the exact Riemann solver, or some other distinctly robust Riemann solver, in a single numerical method. To demonstrate the performance of our approach, it is sufficient to implement it in the first-order Godunov method,[8] which is the building block of high-order Godunov-type schemes. Here we present results for the first-order Godunov method and the Weighted Average Flux (WAF) method,[9] a second-order TVD technique. Other high-order methods can also make use of the present linearized Riemann solver. In fact, for the time-dependent Euler equations the corresponding approach[10] has successfully been used by Quirk[11] in the context of the MUSCL method.

The rest of this paper is organized as follows. Section 2 deals with the governing equations for steady supersonic flow and with the space-marching method. Section 3 presents the linearized Riemann solver for the two-dimensional case. Section 4 contains two-dimensional tests. In Section 5 we extend the linearized Riemann solver to deal with three-dimensional flows. Test problems are also presented. Conclusions and further developments are dealt with in Section 6.

2. SPACE MARCHING

The steady supersonic Euler equations can be used to simulate a good variety of flow situations. The equations are hyperbolic in the flow direction and thus space-marching methods can be deployed directly to evolve the solution downstream.

2.1. Governing equations

The three-dimensional steady supersonic Euler equations in Cartesian co-ordinates are

$$F_x + G_y + H_z = 0, \tag{1}$$

where the vector-valued flux functions are

$$F = \begin{bmatrix} \rho u \\ \rho u^2 + p \\ \rho uv \\ \rho uw \\ u(E+p) \end{bmatrix}, \quad G = \begin{bmatrix} \rho v \\ \rho uv \\ \rho v^2 + p \\ \rho vw \\ v(E+p) \end{bmatrix}, \quad H = \begin{bmatrix} \rho w \\ \rho uw \\ \rho vw \\ \rho w^2 + p \\ w(E+p) \end{bmatrix}. \tag{2}$$

Here ρ is the density, p is the pressure, u, v and w are the x-, y- and z-components of velocity respectively and E is the total energy given by

$$E=\tfrac{1}{2}\rho(u^2+v^2+w^2)+\rho e, \tag{3}$$

where $e=e(\rho, p)$ is the specific internal (or intrinsic) energy, which for ideal gases has the simple expression

$$e=e(\rho, p)=p/(\gamma-1)\rho, \tag{4}$$

with γ denoting the ratio of specific heats.

Computationally, the three-dimensional equations may be treated via the method of fractional steps,[12] which is a sequence of pseudo-two-dimensional problems. The basic algorithm therefore relies on the two-dimensional case

$$F_x+G_y=0, \tag{5}$$

with flux functions

$$F=\begin{bmatrix} \rho u \\ \rho u^2+p \\ \rho uv \\ u(E+p) \end{bmatrix}, \qquad G=\begin{bmatrix} \rho v \\ \rho uv \\ \rho v^2+p \\ v(E+p) \end{bmatrix}. \tag{6}$$

Since discontinuous solutions such as shock waves and slip surfaces are to be admitted, we replace the differential form (5) by the more general integral form

$$\oint (F\,\mathrm{d}y-G\,\mathrm{d}x)=0. \tag{7}$$

The integral is to be evaluated over the boundary of the appropriate control volume. In numerical methods this will be a computational cell.

2.2. *Space marching via conservative methods*

Equations (5) are a set of hyperbolic conservation laws provided that the flow is supersonic, i.e. if the Mach number M is greater than unity, where

$$M=[(u^2+v^2)/a^2]^{1/2} \tag{8}$$

and a is the sound speed given by

$$a=\sqrt{(\gamma p/\rho)}. \tag{9}$$

Consider the computational set-up of Figure 1. Data are given along $x=x_n$ and we propose to evolve the solution in the x-direction to position x_{n+1}. A computational cell i has dimensions Δx by Δy, where the cell width Δy is chosen on accuracy and computational grounds and the step size Δx is chosen on stability grounds. Direct evaluation of (7) over the control volume ABCD of Figure 1 gives

$$F_i^{n+1}=F_i^n+\frac{\Delta x}{\Delta y}(G_{i-1/2}-G_{i+1/2}), \tag{10}$$

where $G_{i+1/2}$ is the numerical approximation to the physical flux function G at the interface between cells i and $i+1$. Having obtained the updated vector F_i^{n+1} according to the conservative scheme (10), one computes the physical variables as follows. First we set

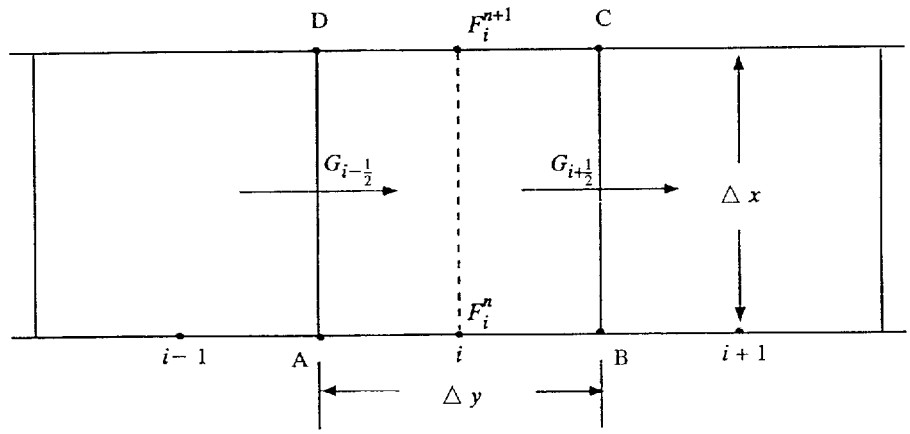

Figure 1. Computational set-up for space marching. Evaluation of conservation laws in control volume ABCD gives explicit, conservative marching procedure

$F_i^{n+1}=[F_1, F_2, F_3, F_4]^T$, with the obvious notation for the components of the updated vector. Manipulations of the four resulting equations give a single quadratic for the density,

$$c_1\rho^2-2c_2\rho-c_3=0, \tag{11}$$

where the coefficients are

$$c_1=(F_3^2/F_1-2F_4)/F_1, \qquad c_2=-\gamma F_2/(\gamma-1), \qquad c_3=(\gamma+1)F_1^2/(\gamma-1). \tag{12}$$

The physically meaningful solution of (11) is

$$\rho=[c_2+(c_2^2+c_1c_3)^{1/2}]/c_1. \tag{13}$$

The other unknowns follow as

$$u=F_1/\rho, \qquad v=F_3/F_1, \qquad p=F_2-F_1^2/\rho, \qquad E=\rho F_4/F_1-p. \tag{14}$$

This completes the space-marching procedure using any conservative method with numerical flux $G_{i+1/2}$.

3. THE LINEARIZED RIEMANN SOLVER

Riemann-problem-based methods use the solution of local Riemann problems to compute the intercell numerical flux $G_{i+1/2}$ in the conservative scheme (10). In this section we present an approximate solution to the Riemann problem.

The solution of the Riemann problem for the two-dimensional steady supersonic Euler equations is depicted in the y–x plane of Figure 2. It is analogous to the time-dependent one-dimensional case; here x is the marching direction. There are three waves present; the left and right waves can be oblique shocks or Prandtl–Meyer expansions, while the middle wave is always a slip line. There are therefore four possible wave patterns.

In carrying out the linearization, there is some freedom in selecting the appropriate variables. Here we select density ρ, velocity components u and v and pressure p. Other possible choices are ρ, flow angle α, Mach number M (or sound speed a) and pressure p. Manipulations of equations

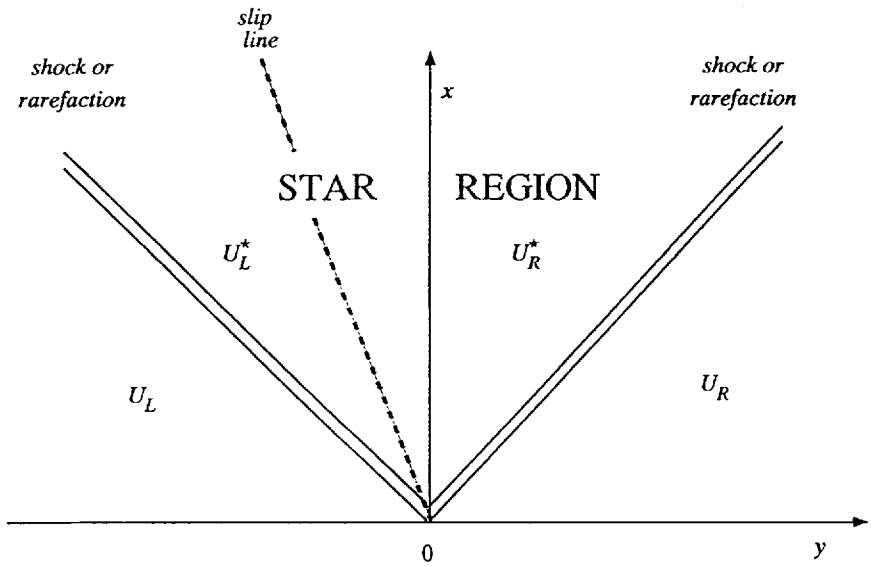

Figure 2. Structure of solution of Riemann problem for steady supersonic Euler equations in y–x plane. There are three waves separating four constant regions. Region *star* is key to solution procedure

(5) and (6) give

$$AW_x + BW_y = 0, \tag{15}$$

where

$$W = \begin{bmatrix} \rho \\ u \\ v \\ p \end{bmatrix}, \qquad A = \begin{bmatrix} u & \rho & 0 & 0 \\ 0 & u & 0 & 1/\rho \\ 0 & 0 & u & 0 \\ 0 & \gamma p & 0 & u \end{bmatrix}, \qquad B = \begin{bmatrix} v & 0 & \rho & 0 \\ 0 & v & 0 & 0 \\ 0 & 0 & v & 1/\rho \\ 0 & 0 & \gamma p & v \end{bmatrix}. \tag{16}$$

It is convenient to express (15) as

$$W_x + CW_y = 0, \qquad C = A^{-1}B, \tag{17}$$

where the matrix C is found to be

$$C = \begin{bmatrix} v/u & -\rho v/d & \rho u/d & v/ud \\ 0 & uv/d & -a^2/d & -v/\rho d \\ 0 & 0 & v/u & 1/\rho u \\ 0 & -\rho v a^2/d & \rho u a^2/d & uv/d \end{bmatrix}, \tag{18}$$

with $d = u^2 - a^2$. The eigenvalues of C are

$$\lambda_1 = \frac{uv - a^2 q}{d}, \qquad \lambda_2 = \frac{v}{u} = \lambda_4, \qquad \lambda_3 = \frac{uv + a^2 q}{d}, \tag{19}$$

where $q = (M^2 - 1)^{1/2}$ is assumed real (flow is supersonic) for hyperbolicity. The corresponding

right eigenvectors are

$$R_1=\begin{bmatrix} -\rho(v-uq) \\ -(a^2q-uv) \\ -(u^2-a^2) \\ -\rho a^2(v-uq) \end{bmatrix}, \quad R_2=\begin{bmatrix} \rho \\ u \\ v \\ 0 \end{bmatrix}, \quad R_4=\begin{bmatrix} \rho v \\ u \\ v \\ 0 \end{bmatrix}, \quad R_3=\begin{bmatrix} \rho(v+uq) \\ -(a^2q+uv) \\ u^2-a^2 \\ \rho a^2(v+uq) \end{bmatrix}. \tag{20}$$

We now assume a local linearization of system (17) so that the coefficient matrix C is a constant matrix that can be expressed in terms of the data left and right of the initial discontinuity. This is accomplished by assuming average values $\bar{r}$, where r is any of the components of the vector W. The objective is to find the complete solution in the *star* region shown in Figure 2. Using standard techniques for linear hyperbolic systems,[13] we find the solution for the Riemann problem explicitly. Use of the generalized Riemann invariants across the left, right and middle waves gives the following set of simultaneous equations for the seven unknowns p^*, u_L^*, v_L^*, ρ_L^*, u_R^*, v_R^* and ρ_R^*:

$$\rho_L^*-p^*/\bar{a}^2=\rho_L-p_L/\bar{a}^2, \tag{21}$$

$$u_L^*+\alpha_1 p^*=u_L+\alpha_1 p_L, \tag{22}$$

$$v_L^*+\alpha_2 p^*=v_L-\alpha_2 p_L, \tag{23}$$

$$\rho_R^*-p^*/\bar{a}^2=\rho_R-p_R/\bar{a}^2, \tag{24}$$

$$u_R^*-\alpha_3 p^*=u_R-\alpha_3 p_R, \tag{25}$$

$$v_R^*-\alpha_4 p^*=v_R-\alpha_4 p_R, \tag{26}$$

$$u_R^*-\bar{u}v_R^*/\bar{v}=u_L^*-\bar{u}v_L^*/\bar{v}, \tag{27}$$

where

$$\alpha_1=\frac{\bar{a}^2\bar{q}+\bar{u}\bar{v}}{\bar{\rho}\bar{a}^2(\bar{v}+\bar{u}\bar{q})}, \quad \alpha_2=\frac{\bar{u}^2-\bar{a}^2}{\bar{\rho}\bar{a}^2(\bar{v}+\bar{u}\bar{q})}, \quad \alpha_3=\frac{\bar{a}^2\bar{q}-\bar{u}\bar{v}}{\bar{\rho}\bar{a}^2(\bar{v}-\bar{u}\bar{q})}, \quad \alpha_4=\frac{\bar{u}^2-\bar{a}^2}{\bar{\rho}\bar{a}^2(\bar{v}-\bar{u}\bar{q})}. \tag{28}$$

It is convenient to solve for p^* first. We do this by taking equation (27) and substituting each of its four unknowns in terms of p^* using the previous equations. The complete result is

$$p^*=\frac{(v_R-v_L+\alpha_2 p_L-\alpha_4 p_R)-\bar{v}(u_R-u_L-\alpha_1 p_L-\alpha_3 p_R)/\bar{u}}{\alpha_2-\alpha_4+\bar{v}(\alpha_1+\alpha_3)/\bar{u}}, \tag{29}$$

$$\rho_L^*=\rho_L+(p^*-p_L)/\bar{a}^2, \tag{30}$$

$$\rho_R^*=\rho_R+(p^*-p_R)/\bar{a}^2, \tag{31}$$

$$u_L^*=u_L+\alpha_1(p_L-p^*), \tag{32}$$

$$u_R^*=u_R+\alpha_3(p^*-p_R), \tag{33}$$

$$v_L^*=v_L+\alpha_2(p^*-p_L), \tag{34}$$

$$v_R^*=v_R+\alpha_4(p^*-p_R). \tag{35}$$

As average values of $\bar{r}$ we take

$$\bar{r}=\tfrac{1}{2}(r_L+r_R) \quad \text{for } r=\rho,\ u,\ v,\ p,\ a, \qquad \bar{q}=[(\bar{u}^2+\bar{v}^2)/\bar{a}^2-1]^{1/2}. \tag{36}$$

Other choices are of course possible, but these are the simplest and for slowly varying data are sufficiently accurate, as we shall see in later sections. It is interesting to note that for the case of an

isolated slip line, i.e. for $p^* = p_L = p_R$, the present linearization is exact, regardless of the choice of average values. One could try a selection of average values so as to exactly recognize isolated shock waves or isolated Prandtl–Meyer expansion waves, but this, if possible at all, might produce computationally expensive expressions.

4. TEST PROBLEMS

There are essentially two ways of assessing the performance of the present linearization. One is by direct comparison of the *star* values (29)–(35) with those given by the exact solution. The second, and perhaps the most relevant to CFD, is by using the linearization in the computation of intercell fluxes $G_{i+1/2}$ in Godunov-type space-marching methods.

4.1. The star values

Here we take two test problems. The variables used are ρ, u, p and flow angle α, which is derived from approximate values of other variables. Table I contains the data values for the two test problems.

Table II gives a comparison of results for tests 1 and 2 with the exact solution and the percentage error. Results are assessed in terms of pressure, density and Mach number.

The significance of the Riemann problem is its local use for intercell flux evaluation in conservative numerical methods of the form (10). Experience shows that very large errors in the *star* values, of the order of 100%, are permitted before these errors begin to affect the numerically computed solution. It is in this context that the errors of Table II should be interpreted, where the maximum error of 7% can be regarded as satisfactory. It must be emphasized, however, that both tests are representative of flows with slowly varying data, the kind of data for which the present linearization is expected to be valid. For severe flow regimes we suggest the use of other more robust Riemann solvers (e.g. an exact Riemann solver) in an adaptive fashion. This can be implemented in a similar way as done by Toro[14] for the time-dependent Euler equations.

Table I. Data for tests 1 and 2

	ρ_L	u_L	p_L	α_L	ρ_R	u_R	p_R	α_R
Test 1	2·0	2·0	2·0	90·0	1·0	2·0	1·0	90·0
Test 2	2·0	2·0	2·0	85·0	1·0	2·0	1·0	95·0

Table II. Comparison of results for tests 1 and 2

		P^*	ρ_L^*	ρ_R^*	M_L^*	M_R^*
Test 1	Exact	1·399	1·550	1·270	1·923	1·459
	Present	1·500	1·643	1·357	1·937	1·478
	Error	7·1%	6·0%	6·8%	0·7%	1·3%
Test 2	Exact	1·074	1·282	1·052	2·100	1·649
	Present	1·115	1·368	1·082	2·160	1·633
	Error	3·7%	6·7%	2·8%	2·8%	1·0%

4.2. Numerical tests in two dimensions

In this subsection we assess the accuracy of the linearized Riemann solver in the context of Godunov-type numerical methods for solving the general initial value problem for the non-linear equations (15) or (17). We use two such numerical methods, namely the first-order Godunov method[8] and the WAF method,[9] a second-order TVD scheme of the Godunov type. As a test problem in two dimensions we consider a Riemann problem, the analogue of a shock tube problem in time-dependent gas dynamics. Problems of this kind have exact solutions which can be used to assess the performance of numerical schemes. We choose a domain $-\frac{1}{2} \leqslant y \leqslant \frac{1}{2}$ and initial data 1·0, 2·28, 1·0 and 90·0° for ρ, u, p and flow angle α respectively to the left of $y = 0{\cdot}0$, and 0·5, 3·35, 0·25 and 90·0° as values for positive y; $\gamma = 1{\cdot}4$; $\Delta y = 0{\cdot}01$ and Δx is chosen from

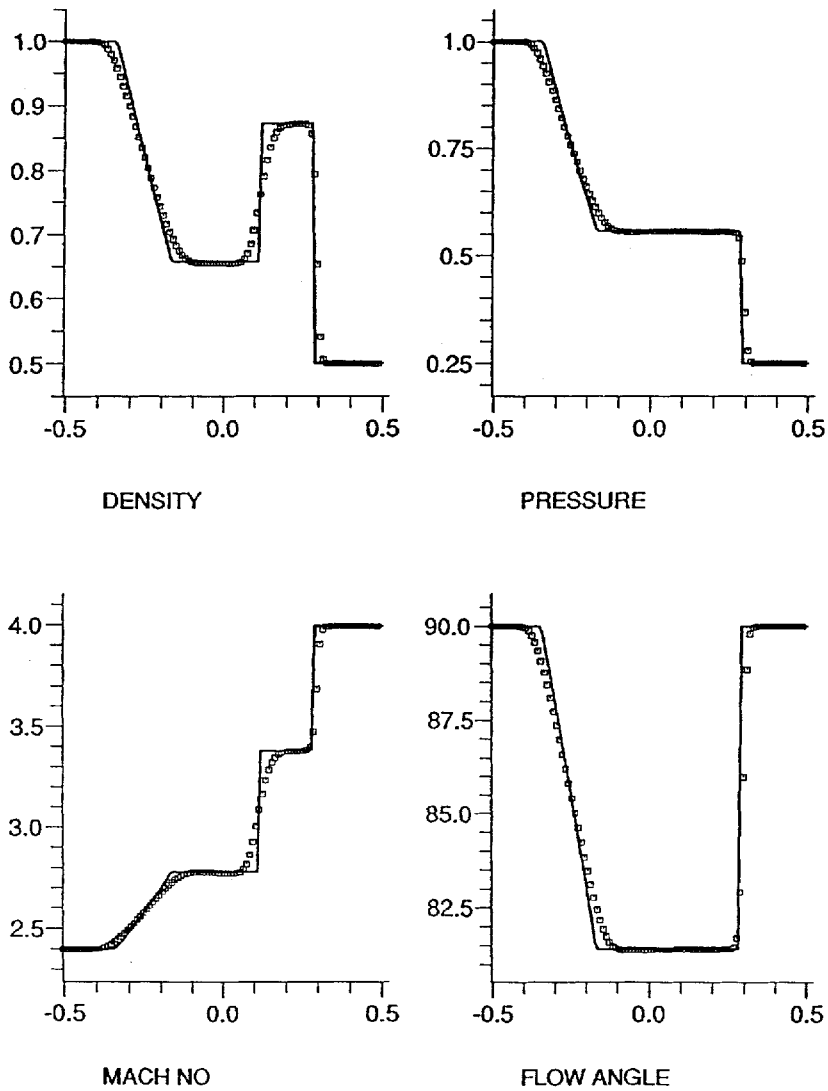

Figure 3. Comparison between exact (line) and numerical (symbol) solutions for a Riemann problem test. The numerical solution was obtained by the Godunov method using the linearized Riemann solver. Compare with Figures 4 and 5

a Courant-like condition with Courant number coefficient 0·8. Transmissive boundary conditions are imposed at both ends.

Figure 3 shows a comparison between the exact solution (line) and the computed solution (symbol) using Godunov's method together with the linearization (11)-(17) alone. The profile shown is that at $x=0{\cdot}75$ downstream. This problem involves a shock wave, a slip line and a Prandtl–Meyer expansion. As expected from Godunov's method, poor resolution of the main features of the solution can be observed. Figure 4 shows the corresponding solution using Godunov's method together with the exact Riemann solver. To plotting accuracy, the numerical solution of the linearized Riemann solver is indistinguishable from that obtained using the exact

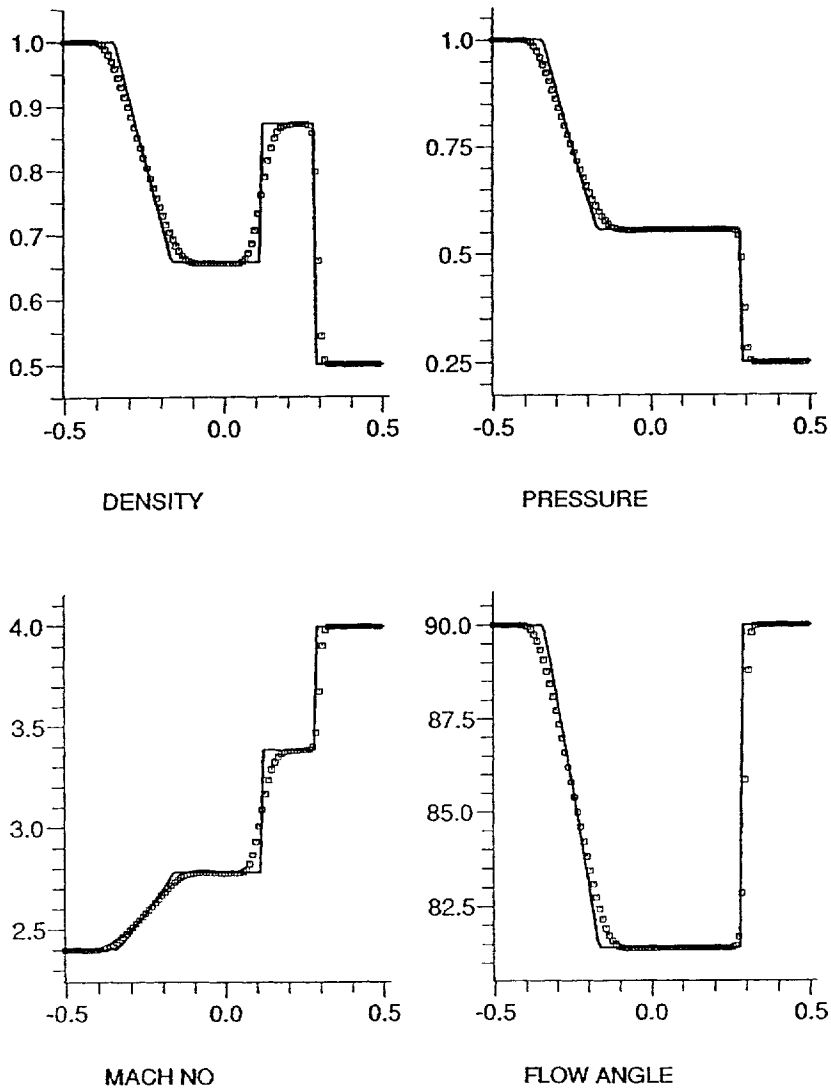

Figure 4. Comparison between exact (line) and numerical (symbol) solutions for a Riemann problem test. The numerical solution was obtained by the Godunov method using the exact Riemann solver. Compare with Figures 3 and 5

Riemann solver. Moreover, in this test the computing time for Godunov's method with the exact Riemann solver is four times that for Godunov's method with the linearized Riemann solver.

Figure 5 shows the result using the WAF method with the linearized Riemann solver. The quality of the solution is improved all round. The head and tail of the expansion are more accurately defined; the shock wave is now resolved with only two interior points as opposed to four or five in the Godunov method. The improvement in the resolution of the slip line is even more evident, from 13 interior points in the Godunov method to three interior points in the WAF method.

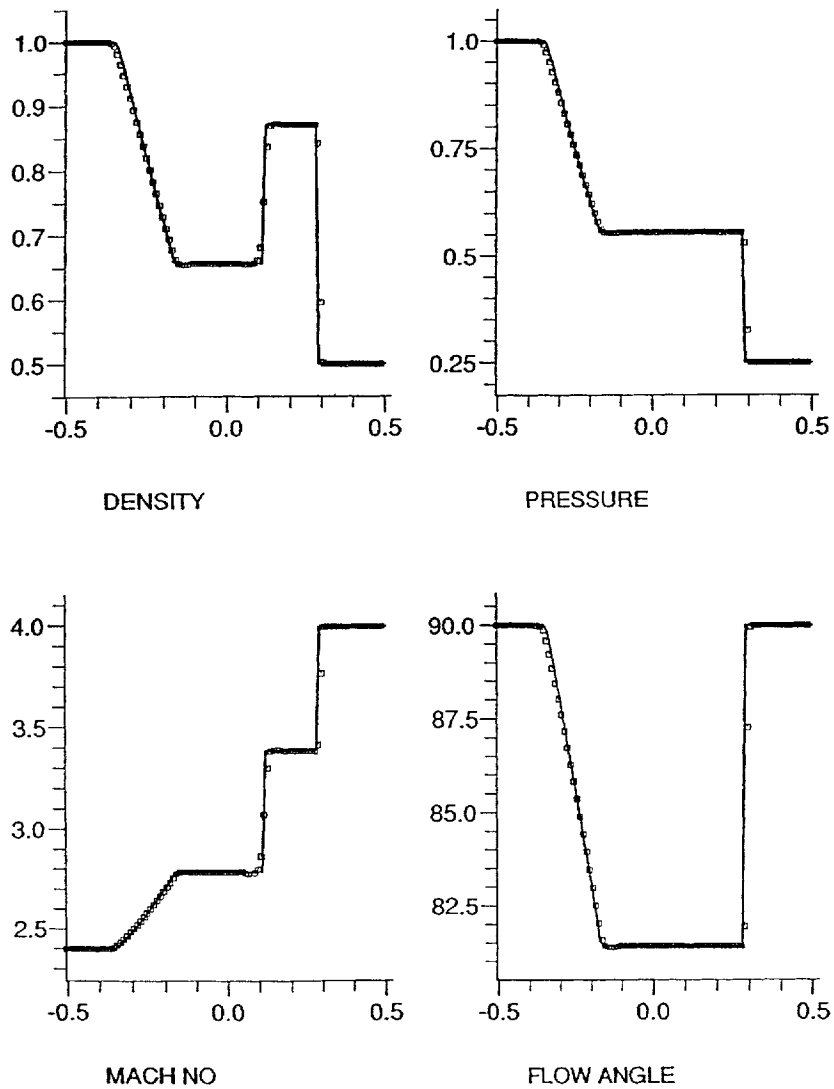

Figure 5. Comparison between exact (line) and numerical (symbol) solutions for a Riemann problem test. The numerical solution was obtained by the WAF method using the linearized Riemann solver. Compare with Figures 3 and 4

The numerical results support the observation made previously that appreciable errors in the computation of the star values in the local Riemann problem do not show at all when used in Godunov-type numerical methods.

5. THREE-DIMENSIONAL FLOW

Numerically, the three-dimensional equations (1) are solved either by operator splitting or by the finite volume method. In both cases one computes pseudo-two-dimensional fluxes in the direction normal to cell boundaries. Thus for each cell interface we only need consider the split three-dimensional case in its normal direction. For simplicity we assume Cartesian geometries and select the y-direction for the purpose of illustrating the method. The treatment of the z-direction is analogous. The split three-dimensional case in the y-direction reads

$$W_x + CW_y = 0, \tag{37}$$

where the coefficient matrix C is given by

$$C = \begin{bmatrix} v/u & -\rho v/d & \rho u/d & 0 & v/du \\ 0 & uv/d & -a^2/d & 0 & -v/d\rho \\ 0 & 0 & v/u & 0 & 1/\rho u \\ 0 & 0 & 0 & v/u & 0 \\ 0 & -\rho v a^2/d & \rho u a^2/d & 0 & uv/d \end{bmatrix}.$$

The eigenvalues λ_1 and λ_3 are as before and $\lambda_2 = \lambda_4 = \lambda_5 = v/\mathrm{u}$. The corresponding right eigenvectors are

$$R_1 = \begin{bmatrix} -\rho(v-uq) \\ -(a^2q-uv) \\ -(u^2-a^2) \\ 0 \\ -\rho a^2(v-uq) \end{bmatrix}, \quad R_2 = \begin{bmatrix} \rho \\ u \\ v \\ w \\ 0 \end{bmatrix}, \quad R_3 = \begin{bmatrix} \rho v \\ u \\ v \\ \rho w \\ 0 \end{bmatrix}, \quad R_4 = \begin{bmatrix} \rho uw \\ u \\ v \\ \rho vw \\ 0 \end{bmatrix}, \quad R_5 = \begin{bmatrix} \rho(v+uq) \\ -(a^2q+uv) \\ u^2-a^2 \\ 0 \\ \rho a^2(v+uq) \end{bmatrix}.$$

It is easily seen that the solution to the Riemann problem with the linearization proposed in Section 4 gives exactly the same solution as that of equations (29)–(35) with the addition

$$w = \begin{cases} w_{\mathrm{L}} & \text{if } y/x \text{ lies to the left of the slip line,} \\ w_{\mathrm{R}} & \text{otherwise.} \end{cases}$$

For the z-direction the problem is the mirror image of that for the y-direction, with the roles of the velocity components v and w interchanged.

5.1. Test problem

As a three-dimensional test problem we choose initial conditions as shown in Figure 6. The inner high-pressure region has data 1·0, 3·35, 0·0, 1·0 and 90·0° for ρ, u, w, p and flow angle α respectively, while for the outer region we take initial values 0·5, 2·82, 0·0, 0·25 and 90·0°. The mesh used has $\Delta y = \Delta z = 0{\cdot}01$ and Δx is chosen from a Courant number coefficient of 0·8. This problem does not have an exact solution but the solution is expected to be symmetric. Also, for some distance downstream the problem remains two-dimensional in the neighbourhood of the centrelines and exact results can be used to test the numerical solution. Transmissive boundary conditions are used throughout.

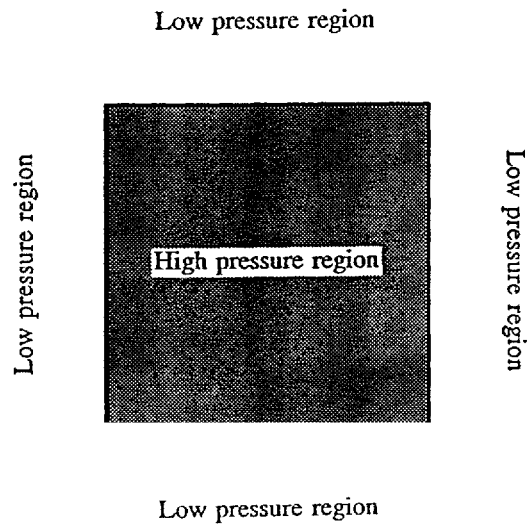

Figure 6. Computational domain and initial data configuration for three-dimensional test problem. Pressure and density are high in inner square

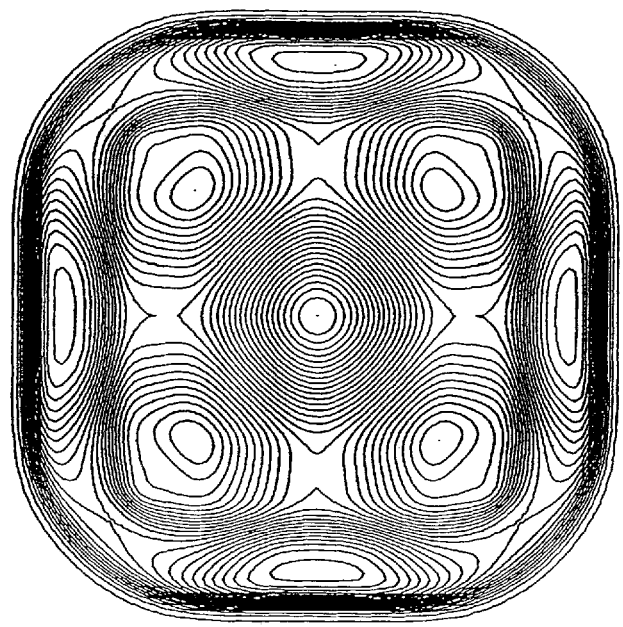

Figure 7. Computed density contours at distance $x = 0{\cdot}45$ downstream. Godunov method is used. Compare with Figure 8

Figure 7 shows the solution at $x = 0{\cdot}45$ downstream obtained by the Godunov method. As expected from the first-order method, the sharp flow features are badly smeared. Figure 8 shows the corresponding solution obtained by the WAF method with a MINMOD-type limiter function; a significant improvement in resolution is observed. For this problem we use the linearized Riemann solver together with the exact Riemann solver adaptively.

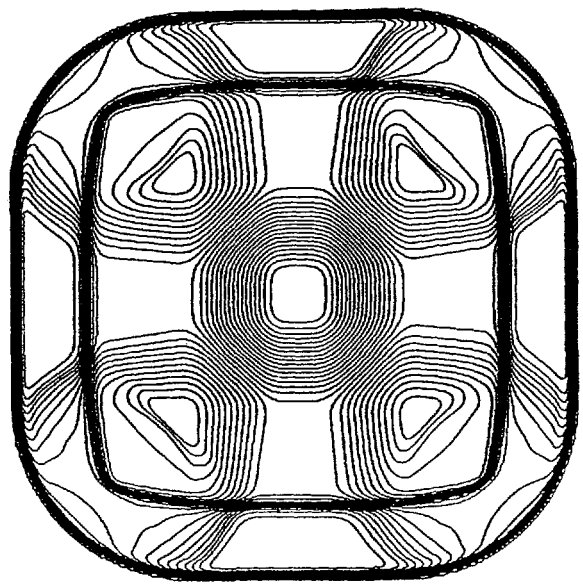

Figure 8. Computed density contours at distance $x=0{\cdot}45$ downstream. WAF method is used. Compare with Figure 7

6. CONCLUDING REMARKS

A linearized Riemann solver for the steady supersonic Euler equations has been presented. This has been applied, together with two Godunov-type methods, to solve test problems in two and three dimensions. The resulting computing savings are significant. The CPU time saving factors are four for the first-order Godunov method and three for the WAF method.

The linearized Riemann solver is not expected to be robust enough for flows containing strong shock waves. For such flows we advocate the use of the present Riemann solver together with the exact Riemann solver, or some other robust solver, in an adaptive fashion.[14] Applications indicate that for severe flow regimes, and depending on the mesh size, the linearized Riemann solver is used to solve over 99% of all Riemann problems. This means that the resulting adaptive algorithms retain the efficiency of the linearized Riemann solver presented in this paper and the accuracy and robustness of the exact Riemann solver.

REFERENCES

1. P. L. Roe, 'Characteristic-based schemes for the Euler equations', *Ann. Rev. Fluid Mech.*, **18**, 337–365 (1986).
2. M. Pandolfi, 'Computation of steady supersonic flows by a flux difference splitting method', *Comput. Fluids*, **10**, 37–46 (1985).
3. R. Marsilio and M. Pandolfi, 'An upwind 3D space-marching procedure', in B. Engquist and B. Gustafsson (eds), *Proc. Third Int. Conf. on Hyperbolic Problems*, Vol. II, Studentliteratur, Uppsala, 1990, pp. 715–726.
4. E. F. Toro, 'Riemann problems and the WAF method for solving the two-dimensional shallow water equations', *Philos. Trans. R. Soc. Lond. A*, 338, 43–68 (1992).
5. D. Hänel, 'On the numerical solution of the Navier–Stokes equations for compressible fluids', *VKI Lecture Series on Computational Fluid Dynamics*, 1989.
6. E. F. Toro and R. E. Brown, 'The WAF method and splitting procedures for viscous shocked flows', *Proc. 18th Int. Symp. on Shock Waves*, Tohoku University, Sendai, July 1991.
7. P. L. Roe, 'Approximate Riemann solvers, parameter vectors and difference schemes', *J. Comput. Phys.*, **43**, 357–372 (1981).

8. S. K. Godunov, 'A finite difference method for the numerical computation of discontinuous solutions of the equations of fluid dynamics', *Mat. Sb.*, **47**, 357–393 (1959).
9. E. F. Toro, 'A weighted average flux method for hyperbolic conservation laws', *Proc. R. Soc. Lond. A*, **423**, 401–418 (1989).
10. E. F. Toro, 'A linearised Riemann solver for the time-dependent Euler equations of gas dynamics', *Proc. R. Soc. Lond. A*, **338**, 683–693 (1991).
11. J. J. Quirk, 'An alternative to unstructured grids for computing gas dynamic flows around arbitrarily complex two-dimensional bodies', *ICASE Rep. 92–7*, NASA Langley Research Center, February 1992.
12. N. N. Yanenko, *The Method of Fractional Steps*, Springer, 1971.
13. A. Jeffrey, *Quasilinear Hyperbolic Systems and Waves, Research Notes in Mathematics*, Pitman, 1976.
14. E. F. Toro, 'Riemann-solver adaptation for gas dynamics', in R. Glowinski (ed.), *Proc. Tenth Int. Conf. on Computing Methods in Applied Sciences and Engineering*, Paris, February 1992, Nova Science Publishers Inc., New York, 1991.